View metadata, citation and similar papers at core.ac.uk
brought to you by CORE
provided by SZTAKI Publication Repository

2013 Conference on Control and Fault-Tolerant Systems (SysTol)
October 9-11, 2013. Nice, France

Smart Mini Actuators for Safety Critical Unmanned Aerial Vehicles*

István Réti**, Márk Lukátsi**, Bálint Vanek**, István Gőzse**, Ádám Bakos**, József Bokor**

***Abstract*— The present article details the development steps and experimental results obtained during the development of smart actuators used for mini Unmanned Aerial Vehicles. Unlike the commercial off-the-shelf hobby components, these units are able to measure position, angular rate and current, furthermore with their controlling microprocessors they are capable of establishing two way communication via CAN and FlexRay protocol. They are suitable for safety critical applications, and self diagnostics features are also hosted onboard the actuators to be part of a redundant, distributed control network. The development challenges and experimental results in an example hardware-in-the-loop simulator of an Unmanned Aerial System are discussed in the paper.**

I. INTRODUCTION

The emerging role of Unmanned Aerial Systems (UAS) for both military and civil operations depends on the ability to gain unrestricted access to national airspace ([14], [4]). One of the key issues that must be resolved to open up the skies for UAS is to be able to coexist safely and effectively with current manned operations in the national and international airspace. This includes the ability to follow pilot commands with high fidelity even in the case of component faults. Since current UAVs, with the exception of Predator, Global Hawk and a few other high cost systems, use single string avionics, there is no way of mitigating flight control system component faults during flight ([3]). It is our aim to develop a redundant low-cost avionics system for UAVs ([10], [12]), where hardware redundancy is combined with analytical redundancy to reduce the overall weight and cost, but take advantage of increased computational performance onboard the aircraft.

The avionics system is based on the philosophy, that in most situations a carefully selected set of built-in-tests and proper handing over protocols between parallel channels can provide the necessary reliability figures ([16]). In case two flight control computers are used and one fails the other will be able to clearly identify the event of a fault in almost all situations if we assume the failed node is transmitting random messages not intentionally trying to attack the rest of the system. The system architecture developed in SZTAKI (Computer and Automation Research Institute of the Hungarian Academy of Sciences) can be seen in Fig. 6. It consists of two independent flight control computers, two INS/GPS sensor units, the three major motion axes are controlled by pairs of independent flight control surfaces, the aircraft has two engines with their own dedicated batteries, two independent electrical power sources are fed to each avionics component and the avionics components are interconnected with a safety critical FlexRay communication bus ([11]). The overall architecture, in its simplest form consists of 12 smart units, each having its own computational capability, which allows to transmit two directional messages between Flight Control Computers (FCC) and actuators ([10]). In conventional small size UAV applications the FCC only sends analog commands to the actuators and might receive an analog feedback from a position sensor about the current status of the unit. In our approach the FCC sends commands over a digital channel to the actuators, where the smart unit takes care of the internal control tasks of servo control and Pulse Width Modulation (PWM) control of the DC motor inside the actuator. Besides the local control tasks the unit is also capable of providing fault detection capabilities ([15]), since position, back electromotive force[1] and drawn current are all measured and using the mathematical model of the actuator analytic parity relations can be used to identify anomalous behavior.

FlexRay communication protocol is selected to provide interconnection between the nodes due to its low cost and the availability of development tools ([12]). A consortium including BMW, DaimlerChrysler, Motorola, and Philips, has developed FlexRay for powertrain and chassis control in cars. It differs from conventional buses like CAN or LIN, since its operation is divided between time-triggered and event-triggered activities. Published descriptions of the FlexRay protocols and implementation are described in ([11]). In both cases, duplication of the interconnect is optional. Each FlexRay interface (it is called a communication controller) drives the lines to its interconnects through separate bus guardians located with the interface. (This means that with two buses, each node has three clocks: one for the controller and one for each of the two guardians; this differs from the bus configuration of TTA, an alternative time-triggered protocol ([9]), where there is one clock for the controller and both guardians share a second clock.) Like the bus configuration of TTA, the guardians of FlexRay are not fully independent of their controllers.

II. DESIGN CONSIDERATIONS

It is practical to develop custom servos with the same form factor as the standard ones available because the

*The research leading to these results has received funding from the European Union Seventh Framework Programme (FP7/2007- 2013) under grant agreement no. 284915. This work is also supported by the Control Engineering Research Group of HAS at Budapest University of Technology and Economics.

**Systems and Control Laboratory, Computer and Automation Research Institute Hungarian Academy of Sciences, Budapest, Hungary.

[1]Back EMF is the voltage induced by the motor, when no current is drawn (no voltage is applied), from which RPM can also be measured at high rotation rate.

Fig. 1. Futaba S3305 COTS RC servo and the custom servo with measurement and power electronics.

gearbox, housing and DC motor can be re-used. On the other hand the onboard electronics of a COTS servo is a black box for the user, hence it cannot be modified for research purposes. Moreover, they do not satisfy the requirements of a modern, reliable UAV, as they are built from a few standard components with minimum 'intelligence' in their control logics:

- The control is done with a dedicated printed circuit board, in this form there is no way of modifying its behaviour
- Servo shaft angle (motor shaft after the reduction gears) is measured with a potentiometer which physically limits displacement and has a high level of noise
- Induced voltage of the motor is not measured
- Voltage regulation is done via a MOSFET bridge
- The reference signal is implemented with a $0 - 5$ V level PWM input, this corresponds to a 50 Hz frequency square wave signal with different pulse widths. Maximum displacement is commanded with 1 ms long high and 19 ms long low signal value, while negative sign maximum displacement is achieved with 2 ms long high signal level.
- The difference between maximum and minimum displacement is less than 270 degrees, limited by the mechanical construction of the potentiometer
- Communication with the environment is one-way, via the PWM signal.

Due to the aforementioned limitations, COTS servos are not applicable for modern UAVs. The custom made servo has to satisfy the following performance requirements:

- Independent, self-contained operation with multiple cascade control-loops, reference tracking with sufficient bandwidth and zero steady state error
- The control-loop parameters should be tunable, to achieve different desired responses
- To satisfy the model based control and fault detection requirements, the model parameters should be measured or identified
- All the measurable quantities should be available for diagnostic purposes, to provide the highest number of analytically redundant data
- Self-testing and self-diagnostics should be implemented
- High-level, two-way communication via the FlexRay (or at least CAN) bus should be used for real-time, fault tolerant performance
- The lifespan of the servo due to customization should not be compromised

The first task is to select a suitable servo type for modification. The three main requirements are precision, maximum torque and lifespan. Since only the housing, gears and the motor is used in the modified servo, these requirements pointed towards a unit with metal gears, small backlash and with sufficient space in the housing. The motor should be coreless, since it is free from the reluctance type torque disturbances, which makes the characteristics of the motor magnetic field nonlinear around small torques, undesirable for control purposes. We used a COTS Futaba S3305 RC servo [7] as a baseline, which is modified during the development of the custom actuator unit as shown in Fig. 1. This has a non-coreless motor, but the gears are metal with minimal backlash. In a later stage of development we will consider to replace it by a coreless one.

In the second stage of the development, the electronics modules of the unit are developed. According to the specification, the servo should be able to communicate via the FlexRay [11] bus. Since this communication protocol is not widespread in the industry, due to its maturity, only a limited set of microcontrollers have communication controllers built into them supporting the FlexRay protocol. Our choice was to use the Freescale S12XF512 microcontroller, which has a development environment and available not only for automotive customers. This unit is a relatively large integrated circuit, with 112 legs, which is larger than the size of the servo housing, hence the complete electronics is done in two separate components. The board housing the sensors, power electronics and the control electronics is placed inside the servo unit, while the board containing the S12XF microcontroller is outside the box, connected via a dedicated cable, as shown in Fig. 3. The module containing the microcontroller is designed to be able to control not only the servos but the large BLDC electrical engines of the aircraft via their dedicated power electronics. The units also have a CAN bus communication link [8] which can be used for the same purpose as FlexRay if safety critical

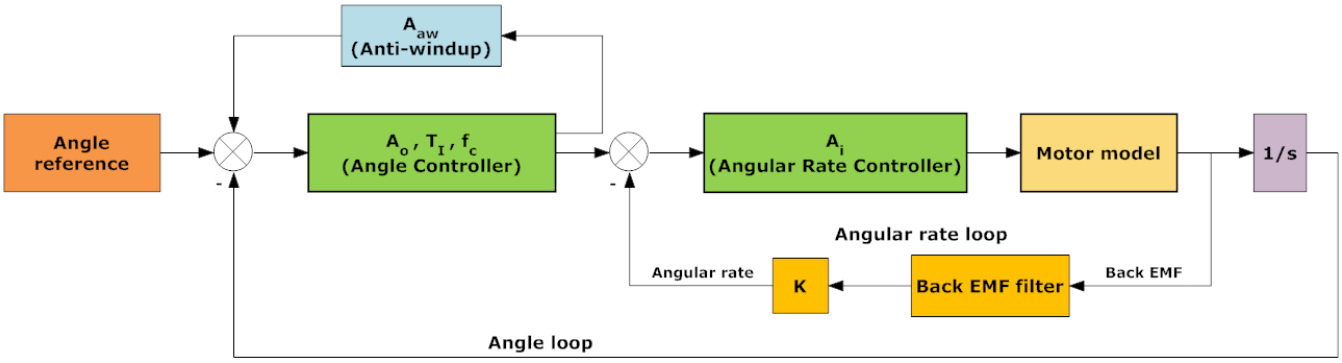

Fig. 2. Architecture of the modified PI controller with feedforward of the command signal.

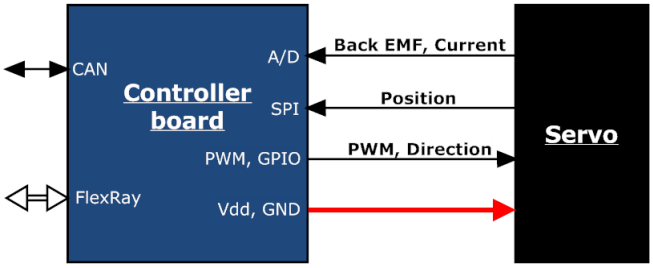

Fig. 3. Block scheme of the servo mechanism.

communication is not necessary. The electronics inside the servo contains the following components:

- Sensor for the angle measurement of the servo shaft
- Circuit, including signal conditioning and amplification, of the induced voltage measurement in the motor
- Circuit, including signal conditioning and amplification, of the current measurement inside the motor
- The MOSFET bridge, controlling the motor voltages, with its driving circuit

The magnetic rotary encoder, which measures shaft position is the Austria Micro Systems AS5045 unit which is a system on a chip solution for Hall-element sensing. The analog amplification and digital signal processing is done on the unit, measurement are sent via an SPI communication bus. It allows contactless angle measurement with 12 bit resolution leading to 0.0875° maximum precision.

The digital input commands are the direction of the rotation and the voltage on the motor and the position of the shaft, the motor current and the ack EMF signals are sent back to the microcontroller board. The supply voltage for the motor and for the electronics are also sent via this cable. The control, fault diagnostics and communication algorithms are implemented on the microcontroller, which has access to all internal and the necessary external signals. The circuit board is capable to connect to a redundant electrical network, via a power switch, which is selecting always the healthier electrical bus with seamless transition.

III. IMPLEMENTATION

A. CONTROL

One of the main goals of the custom servo development is precise position control. To close the position loop in the controller an additional inner angular rate loop based on back EMF measurement is necessary. It is interesting to note, that this signal can be measured only when there is no voltage applied to the motor (at zero PWM level), after the transients. A dedicated logic is determining the required PWM signal and based on the rotation speed the sequence of polarities applied to the motor to maintain the desired rotation direction, since only rate but not the direction is determined by the PWM signal.

The logic behind the control is the following: position control is done with 250 Hz, with position measurement of 250 Hz. The frequency of the PWM signal is 1 kHz, back EMF is measured with this frequency and speed control is also done with 1 kHz. It is also important to note, that back EMF is always measured in the middle of the low PWM level, to reduce the transient effects. Obviously the more the duty cycle is, the more the noise rate of the back EMF measurement has, hence the frequency of the PWM and the duty cycle is limited.

The control is done via two cascade loops, where the inner loop is realized as a P controller and the outer loop as a modified PI controller with feedforward of the command signal [6]. The inner loop is responsible for angular rate while the outer loop for angle reference tracking as shown in Fig. 2 (saturation of angular rate and PWM increments are included in the controller blocks). As a first step, the model of the actuator is identified, using subspace based identification methods. PWM steps are used as input signals, while back EMF, shaft angle and current measurements are used as outputs. The identified model has one dominant and one minor modes, hence a simple first order model is selected for control design purposes:

$$G_{nom} = \frac{2.836}{s + 7.586},$$

where the input of the model is PWM increment, the maximum value of which is 1675 (maximum duty cycle is 67%), while the output is angular rate of the output shaft in °/sec.

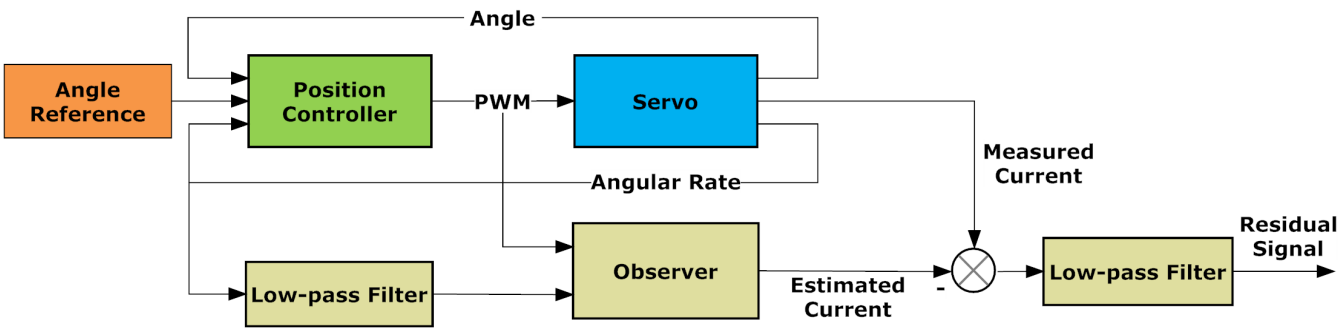

Fig. 4. Block diagram of the Fault Detection Filter

The identification is done around 0 °/sec angular rate, but it is important to note that a maximum angular rate of 420 °/sec is achievable with the design and at higher angular rates the system becomes strongly nonlinear. The detailed description of the control loops and their implementation can be found in [13]. As the inner P controller has steady state error, the saturation limit is 500 °/sec.

B. SENSOR COMPENSATION

Considering the assembly of the magnetic rotary encoder, due to the misalignment of the shafts, a periodic offset error is introduced in angle measurement. To determine the compensation of this cyclic error, first the measured angle have to be unwrapped and detrended. In this signal there is a periodical component, and its period equals to one turn of the shaft [13]. To remove this offset a polynomial is fitted and subtracted from the original signal. After a sufficient number of measurements, within the confidence interval of the periodic errors, the most likely offset values - for a complete turn - are obtained by averaging. Finally quantization is needed, to get sensor increment dimension for software implementation. After compensation, the control characteristics are only slightly affected, however the absolute position measurement is improved from $2°$ RMS value down to a significantly lower $0.15°$.

C. FAULT DIAGNOSTICS

Building a redundant avionics architecture requires an algorithm that identifies the faults of the redundant components. To make the units fully self-contained, this algorithm is also implemented in the microcontroller running the control algorithms. Besides simple range and freeze checks of the signals which can detect obvious fault scenarios (e.g. open-circuit failure of a MOSFET) model-based detection is also implemented to recognize faults that affect the performance in a less abrupt way. One such fault is the partial jamming of a control surface which results in a great increase in motor load. We use a Fault Detection Filter (FDF) as a simple model-based approach to detect this fault mode.

An FDF is based on a full-order state observer, from which the output of the system is reconstructed. This estimated output is subtracted from the measured output and then filtered by a low-pass or band-pass filter, forming the residual signal [5], [2]. If this signal exceeds a predefined threshold an error is signalled.

The inputs of the observer are the PWM signal and the angular rate of the output shaft. The outputs are the estimated angular rate and current, but only the latter is used for the residual generation, bacause the jamming fault mode is associated with increased current consumption.

The model identified in Section III-A can be written into state-space form:

$$\dot{x} = Ax + Bu$$
$$y = Cx + Du$$

where

$$A = \begin{bmatrix} -2.567 & 10.863 \\ -309.344 & -405.718 \end{bmatrix}, B = \begin{bmatrix} 0 \\ 85.628 \end{bmatrix},$$

$$C = \begin{bmatrix} 1 & 0 \end{bmatrix}, D = 0$$

and u is the input voltage in PWM increments, y is the output angular rate in °/sec and the first component of the state vector is the angular rate and the second component is the current. It is worth to note that this model is valid around the trim point of 800 PWM increments and with a 9 V supply voltage. As the maximum PWM duty cycle is 67 % the voltage supply is techniquely 6V.

The system is observable as the observability matrix has rank 2. The observer has the form:

$$\dot{\hat{x}} = A\hat{x} + Bu + L(y - C\hat{x} - Du)$$
$$\hat{y} = C\hat{x} + Du$$

where with the appropriate choice of the observer matrix L the poles of the observer dynamics $(A - LC)$ can be allocated arbitrarily, thus setting the convergence rate of the observer. The poles are chosen to be $[-200, -200.1]$ for sufficient bandwidth, with pole multiplicity of 1 to have a numerically better conditioned result.

To reduce the effect of measurement noise, the angular rate is filtered with a second order low-pass Butterworth filter. Experimental results show, that 5 Hz cutoff frequency is efficient for eliminating the noise, without considerable phase delay. Because of the H-bridge circuit in the power electronics current always flows through the current-sensing resistor

in one direction, regardless of the direction of rotation, so the sign of the measured current must be determined from the sign of the PWM signal. The observer is implemented with 250 Hz sampling frequency on the microcontroller.

The state space representation is transformed into a transfer function and the residual signal is built from the estimated current. To obtain the residual signal the estimated current is subtracted from the measured current and then fed through a low-pass filter with a cutoff frequency of 0.159 Hz to reduce the effect of noise and high-frequency model uncertainties, while maintaining robustness but shortening detection time as much as possible. (Fig. 4).

IV. TEST RESULTS

A. CONTROL

The behaviour of the servo is compared with the COTS servo unit (Futaba S3305) as shown in Fig. 5. The response for a step command of 32° (130 % of the maximum actuator command) is compared. Although the rising time of the custom servo is slightly larger than the COTS's but it has no overshoot. Considering an aerial vehicle, it is an absolute necessity. Neither of them has steady state error, however the COTS can be easily rotated by hand, while the custom servo exerts much higher counterforce, with negligible transient in the position owing to the anti-windup. Tests are made in a hardware-in-the-loop (HIL) test environment of a UAV system, which is used to validate the navigation and control algorithms and the hardware components of the system before flight tests. The environment is used to test the fault tolerant avionics architecture being developed at SZTAKI [1]. The current set-up contains a PC running the dynamic model of the UAV and its environment, two Flight Control Computers (FCCs), three servo actuators and the network interconnecting them [10], [12], [16] shown in Fig. 6. Simulated sensor data is sent to FCCs via a serial link, where navigation and control algorithms are executed and the control commands are sent to the Actuator Control Computers via the FlexRay network. Actual position of the actuators, along with other measurements useful for health monitoring, are sent back to drive the aircraft dynamics. Including the physical actuator dynamics into the system increases the fidelity of the simulation and its effects can be

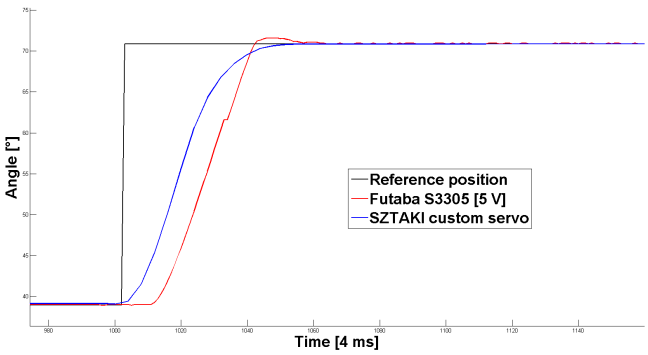

Fig. 5. Comparison of Futaba S3305 and custom servo.

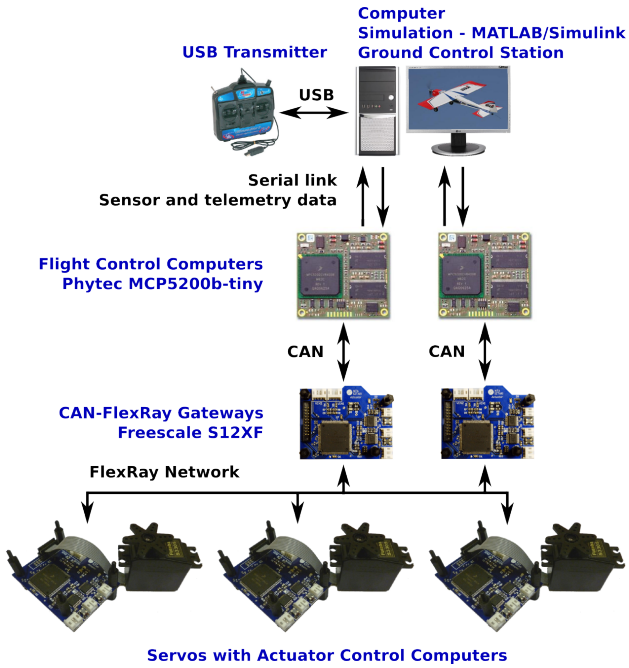

Fig. 6. Hardware-in-the-loop setup for UAV development.

taken into account in the design of the overall flight control algorithms, moreover simulated failures can be injected to test the safety critical aspects of the system.

Actuator deflections in an autonomous waypoint navigation flight are shown in Fig. 7. It can be seen that the reference signal is tracked well and the steady state error is smaller than 0.4°, which is acceptable for flight control purposes.

B. FAULT DIAGNOSTICS

The estimated and measured current in open-loop can be seen on Fig. 8, the motor is controlled around the trim point where the model is identified. In the fault-free case the estimated current is tracking the measured value within approximately 44 mA and when a fault is induced (manual locking of the output shaft) there is a remarkable difference between the signals. Several measurements on different servo units prove the robustness of the observer. Though the observer is designed for the particular servo unit which model is identified, there is no significant difference in tracking errors of other units. The absolute value of the residual is below 11 mA in the fault free case but when a jamming fault is induced it reaches the value of 370 mA in 2.18 s.

To validate the closed loop operation of the filter and to determine the threshold for the jamming fault mode extensive tests are made in the HIL test environment. During a simulation of 21 minutes control demands of the servos are collected and then used as realistic control inputs during the testing and threshold setting of the FDF. The maximum of the absolute value of the residual signal is 77 mA during the whole test in the fault-free case and reached 705 mA when a fault occurred, so a threshold of 100 mA is chosen. It can

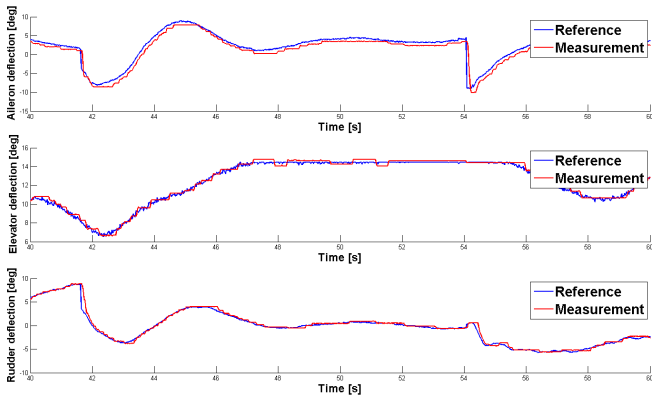

Fig. 7. Actuator deflections in a hardware-in-the-loop simulation.

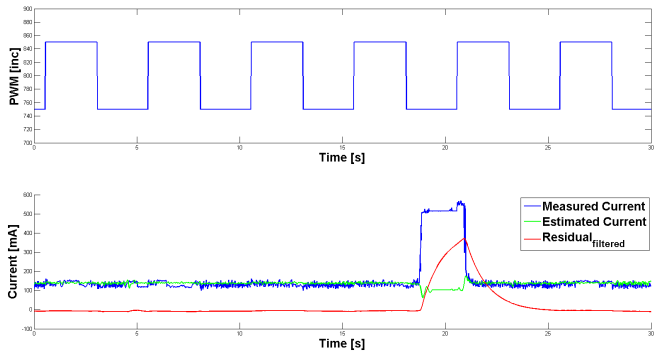

Fig. 8. Operation of the FDF in open loop. The servo is rotating clockwise with 130-145 °/sec. A fault is occuring at 18.74 s

be seen on Fig. 9 that when the fault occurred the residual exceeded the threshold in 0.24 s and dropped below it 2.18 s after the end of the fault. The fault detection algorithm built this way is clearly capable of indicating this fault mode.

V. CONCLUSION

The present article discusses the development of a smart actuator with onboard fault diagnostics with an example application on a small scale Unmanned Aerial Vehicle. The newly developed servo unit builds heavily on the mechanical components of a commercial off-the-shelf remote control servo unit, but its electronics and software are custom designed for the purpose of fault-tolerant safety critical systems. The reasons behind design decisions are discussed and the development steps are detailed in the article, followed by experimental results done on a hardware-in-the-loop test facility. The future steps should include the characterization of dominant fault modes of the actuator, along with determining the reliability figures of the units including mean time between failures and evaluation of the performance of the onboard health monitoring unit (true detection rate, missed detection rate, false alarms).

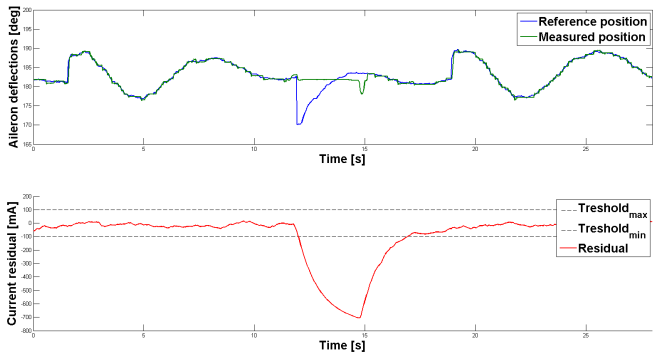

Fig. 9. Operation of the FDF in closed loop with a fault occuring at 11.74 s

REFERENCES

[1] Péter Bauer, Paw Yew Chai, Luigi Iannelli, Rohit Pandita, Gergely Regula, Bálint Vanek, Gary J. Balas, Luigi Glielmo, and József Bokor. UAV Lab, open research platform for unmanned aerial vehicles. In *Advances in aerospace guidance, navigation and control. Selected papers of the 1st CEAS specialist conference on guidance, navigation and control.*, Munich, Germany, 2011.

[2] J. Chen and R.J. Patton. *Robust Model-based Fault Diagnosis for Dynamic Systems*. KLUWER, 1999.

[3] Timothy H. Cox, Christopher J. Nagy, Mark A. Skoog, Ivan A. Somers, and Ryan Warner. Civil uav capability assessment. Technical report, NASA Dryden Flight Research Center, 2004.

[4] M.E. Dempsey. U.s. army unmanned aircraft systems roadmap 2010-2035. Technical report, U.S. Army UAS Center of Excellence, 2010.

[5] Steven X. Ding. *Model-Based Fault Diagnosis Techniques*. Springer, 2008, 2013.

[6] Guillaume J. J. Ducard. *Fault-tolerand Flight Control and Guidance Systems*. Springer, 2009.

[7] Futaba Corp. *S3305 Servo Manual*, 2012.

[8] Robert Bosch GmbH. *CAN Specification Version 2.0*, 1991.

[9] H. Kopetz and G. Bauer. The time-triggered architecture. *Proceedings of the IEEE*, 91(1):112 – 126, jan 2003.

[10] M. Lukátsi. Avionics architecture for safety critical UAVs. Master's thesis, Budapest University of Technology and Economics, 2012.

[11] Adam Opel, Bayerische Motoren Werke, Daimler, Freescale Halbleiter Deutschland, NXP B.V., Robert Bosch, and Volkswagen. *FlexRay Communications System Protocol Specification Version 3.0.1*, 2010.

[12] I. Réti. Design and implementation of a uav onboard communication system. Master's thesis, Budapest University of Technology and Economics, 2012.

[13] István Réti, Márk Lukátsi, Bálint Vanek, István Gőzse, Ádám Bakos, and József Bokor. Smart mini actuators for mobile robots (submitted). In *6th European Conference on Mobile Robots*, Barcelona, Spain, 2013.

[14] United States Government Accountability Office. Unmanned aircraft systems. Technical report, Measuring Progress and Addressing Potential Privacy Concerns Would Facilitate Integration into the National Airspace System, 2012.

[15] Bálint Vanek, Zoltán Szabó, András Edelmayer, and József Bokor. Geometric LPV fault detection filter design for commercial aircrafts. In *AIAA guidance, navigation, and control conference*, Portland, USA, 2011.

[16] T. Varga. Architectural considerations of a safety critical UAV control system. Master's thesis, Budapest University of Technology and Economics, 2011.